PROCEEDINGS OF SPIE

SPIEDigitalLibrary.org/conference-proceedings-of-spie

Automated detection and quantification of Wilms' Tumor 1-positive cells in murine diabetic kidney disease

Darshana Govind, Briana Santo, Brandon Ginley, Rabi Yacoub, Avi Rosenberg, et al.

Darshana Govind, Briana A. Santo, Brandon Ginley, Rabi Yacoub, Avi Z. Rosenberg, Kuang-Yu Jen, Vighnesh Walavalkar, Gregory E. Wilding, Amber M. Worral, Imtiaz Mohammad, Pinaki Sarder, "Automated detection and quantification of Wilms' Tumor 1-positive cells in murine diabetic kidney disease," Proc. SPIE 11603, Medical Imaging 2021: Digital Pathology, 116030F (15 February 2021); doi: 10.1117/12.2581387

SPIE.

Event: SPIE Medical Imaging, 2021, Online Only

Downloaded From: https://www.spiedigitallibrary.org/conference-proceedings-of-spie on 13 Dec 2022 Terms of Use: https://www.spiedigitallibrary.org/terms-of-use

Automated detection and quantification of Wilms' Tumor 1-positive cells in murine diabetic kidney disease

Darshana Govind[1], Briana A. Santo[1], Brandon Ginley[1], Rabi Yacoub[2], Avi Z. Rosenberg[3], Kuang-Yu Jen[4], Vignesh Walavalkar[5], Gregory E. Wilding[6], Amber M. Worral[1], Imtiaz Mohammad[1], Pinaki Sarder[1, *]

[1]Department of Pathology and Anatomical Sciences, [2]Department of Internal Medicine, [6]Department of Biostatistics, University at Buffalo, Buffalo, NY

[3]Department of Pathology, Johns Hopkins University School of Medicine, Baltimore, MD

[4]Department of Pathology and Laboratory Medicine, University of California at Davis, CA

[5]Department of Pathology, University of California San Francisco, San Francisco, CA

[*]Address all correspondence to: Pinaki Sarder
Tel: 716-829-2265; E-mail: pinakisa@buffalo.edu

Abstract

In diabetic kidney disease (DKD), podocyte depletion, and the subsequent migration of parietal epithelial cells (PECs) to the tuft, is a precursor to progressive glomerular damage, but the limitations of brightfield microscopy currently preclude direct pathological quantitation of these cells. Here we present an automated approach to podocyte and PEC detection developed using kidney sections from mouse model emulating DKD, stained first for Wilms' Tumor 1 (WT1) (podocyte and PEC marker) by immunofluorescence, then post-stained with periodic acid-Schiff (PAS). A generative adversarial network (GAN)-based pipeline was used to translate these PAS-stained sections into WT1-labeled IF images, enabling *in silico* label-free podocyte and PEC identification in brightfield images. Our method detected WT1-positive cells with high sensitivity/specificity (0.87/0.92). Additionally, our algorithm performed with a higher Cohen's kappa (0.85) than the average manual identification by three renal pathologists (0.78). We propose that this pipeline will enable accurate detection of WT1-positive cells in research applications.

Key-words (5): WT1-positive cell detection, deep learning, pix2pix GAN, immunofluorescence

I. INTRODUCTION

Podocytes play a key role in maintaining the function of the glomerulus[1]. Podocyte loss has been associated with progressive glomerular damage[2] in diabetic kidney disease (DKD)[3], during which, parietal epithelial cells (PECs) migrate to the tuft, as a coping mechanism[4]. Therefore, the quantification of podocytes and PECs are of high clinical significance. Due to visual similarities to other glomerular cells, there are no automated methods to directly quantify podocytes from brightfield

Medical Imaging 2021: Digital Pathology, edited by John E. Tomaszewski, Aaron D. Ward, Proc. of SPIE Vol. 11603, 116030F · © 2021 SPIE
CCC code: 1605-7422/21/$21 · doi: 10.1117/12.2581387

Downloaded From: https://www.spiedigitallibrary.org/conference-proceedings-of-spie on 13 Dec 2022
Terms of Use: https://www.spiedigitallibrary.org/terms-of-use

images of renal tissue sections. We employed a generative adversarial network (GAN)-based pipeline to translate Periodic acid-Schiff (PAS)-stained renal tissue sections obtained from a mouse model of streptozotocin (STZ) – induced DKD into Wilms' Tumor 1 (WT1)-labeled immunofluorescence (IF) images, enabling *in silico* label-free podocyte and PEC identification in brightfield images. Our method detected WT1-positive cells with high sensitivity/specificity (0.87/0.92). Additionally, our algorithm performed with a higher Cohen's kappa (0.85) than the average manual identification by three renal pathologists (0.78). This pipeline may enable accurate WT1-positive cell detection in research applications.

II. RESULTS

Data generation: Out of 14 mice, 7 were control and 7 were treated with STZ, the latter of which was categorized as mild (200-400 mg/dL) or moderate (>400 mg/dL) diabetes mellitus (DM), based on their fasting blood glucose in the four weeks before euthanasia. Twenty-four tissue sections were stained for WT1 (podocyte and PEC marker) and DAPI, and native IF images captured. These sections were post-stained with PAS counterstained with hematoxylin.

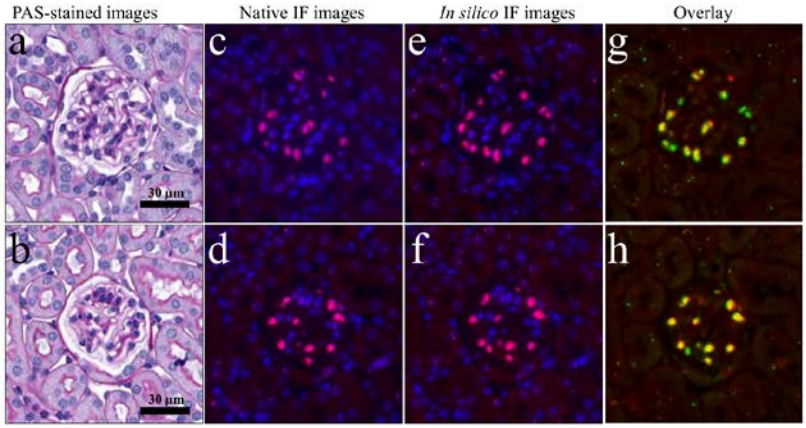

Figure 1. Pix2pix network predictions. (a-b) PAS-stained image patches containing glomeruli, c-d) Native IF-stained image patches containing the same glomeruli as in Figure 1a-b, e-f) *In silico* IF images for these glomeruli, g-h) Overlay of WT1-positive cells from native and *in silico* IF images. The yellow, pure green, and pure red nuclei indicate true positive, false positive, and false negative WT1-positive cells, respectively.

Pix2pix network training and predictions. To train a pix2pix conditional GAN[5], the training images need to be aligned. Therefore, image registration[6] was used to align the PAS and native IF whole slide images (WSIs). Subsequently, the glomeruli from all 24 WSIs (PAS and the registered native IF) were extracted as image patches, using our previously published human-AI-loop (H-AI-L) algorithm[7], and fed to the pix2pix GAN. The model was trained via leave-one-out validation, wherein all the glomerulus patches from one mouse were treated as hold-out cases and trained on the rest, with each of the 14 mice treated as a hold-out case in sequence. Figure 1 shows *in silico* IF images generated by the network from hold-out glomeruli.

Segmentation and comparison of WT1-positive cells with native IF derived ground truth: To analyze the performance of the network, the WT1-positive cells from the *in silico* and the native IF image were segmented into respective masks via morphological processing[8]. We then compared the segmentation results to hand-segmented masks of WT1-positive cells from 10 randomly chosen glomeruli from each of the 24 PAS WSIs. The hand-segmented masks from PAS WSIs were obtained using the native IF image derived WT1-positive cell masks as references. The comparison of the *in silico* segmented cells with ground truth displayed a sensitivity/specificity of 0.87/1.0 for n = 240 glomerulus image patches.

Downloaded From: https://www.spiedigitallibrary.org/conference-proceedings-of-spie on 13 Dec 2022
Terms of Use: https://www.spiedigitallibrary.org/terms-of-use

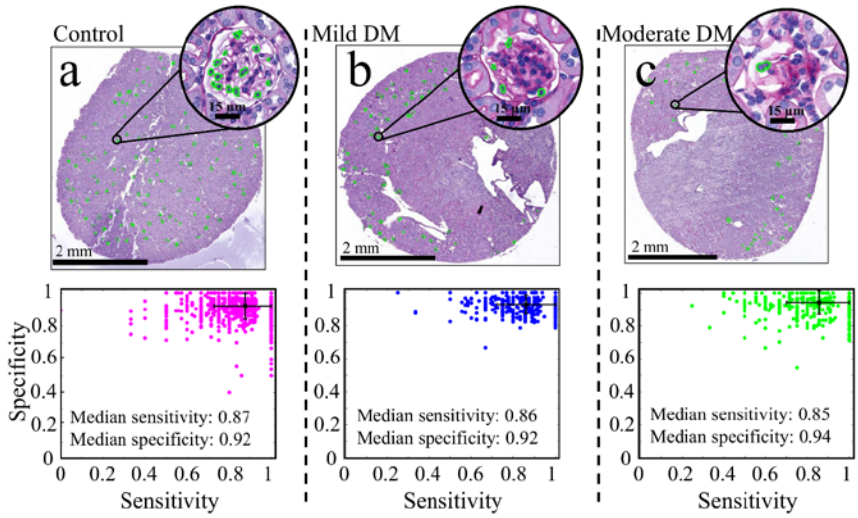

Figure 2. Performance of the pix2pix network in control, mild, and moderate DM. The network predictions of WT1-positive cells (outlined in green) are shown, on control (left), mild (middle), and moderate (right) DM WSIs, along with the median performance metrics (sensitivity, specificity, and accuracy). Error bar signifies one standard deviation along the respective performance metric.

Performance evaluation in control, mild, and moderate DM: The WT1-positive cell masks extracted from the *in silico* IF images were converted into .xml format in Aperio ImageScope (Aperio Technologies, Vista, CA), a widely used WSI-viewing software. The network displayed median hit-or-miss sensitivity/ specificity values of 0.87/0.92, 0.86/0.92, and 0.85/0.94, for control, mild, and moderate DM cases, respectively (Figure 2).

Quantitative analysis: The enumeration of WT1-positive cells from the native and *in silico* IF images showed no significant differences (Pearson's correlation coefficient, $r = 0.83$, with a 95% confidence interval (CI) of [0.81, 0.84]; $p < 0.05$).

Comparison with manual detection of WT1-positive cells: We had three renal pathologists (annotators A1, A2, and A3) manually annotate both podocytes and PECs (in order to maintain consistency between the automated and manual analysis) from 72 randomly chosen PAS image patches. Annotators A1, A2, and A3 displayed strong correlations with the ground truth (native WT1 IF): for A1, $r = 0.77$ with a 95% CI [0.65, 0.85], $p < 0.05$; for A2, $r = 0.73$ with a 95% CI [0.61, 0.83], $p < 0.05$; and for A3, $r = 0.76$ with a 95% CI [0.65, 0.85], $p < 0.05$, whereas, the algorithm displayed a stronger association with the ground truth ($r = 0.89$ with a 95% CI [0.83, 0.93], $p < 0.05$). In order to quantify the agreement between the ground truth and the estimated cell counts, we used a Bland-Altman plot[9] (Figure 3). These results indicate that

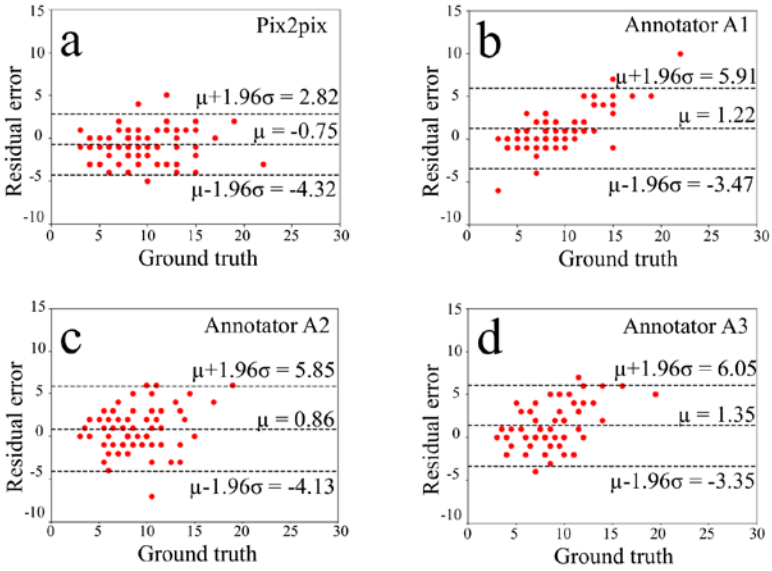

Figure 3. Bland-Altman plots depicting the comparison of detected podocytes. The Bland-Altman plots display the agreement between the ground truth and estimated WT1-positive cell counts by pix2pix, and annotators A1, A2, and A3. a) The residual error and 95% limits of agreement between the ground truth and pix2pix, calculated using the mean (μ) and 1.96 times the standard deviation (σ) of the mean difference between the two measures. b-d) Same as 4a, for annotators A1, A2, and A3, respectively.

Downloaded From: https://www.spiedigitallibrary.org/conference-proceedings-of-spie on 13 Dec 2022
Terms of Use: https://www.spiedigitallibrary.org/terms-of-use

the pix2pix-estimated WT1-positive cell counts are the closest to the ground truth. Overall, all three annotators identified WT1-positive cells with a sensitivity/specificity of (A1) 0.77/0.95, (A2) 0.77/0.94, and (A3) 0.75/0.95, compared to pix2pix (0.92/0.93). Overall, visual screening demonstrated that the major difference in the sensitivity is due to podocytes deep within the glomerulus ("central podocytes"), rather than at the periphery of the glomerular tuft ("peripheral podocytes"). We then calculated the linear weighted Cohen's kappa (κ)[10] values for the annotators and the algorithm, for three classes of nuclei within the glomerulus: 1) peripheral podocytes and PECs, 2) central podocytes, and 3) non-podocyte cells. Annotators A1, A2, and A3 displayed substantial agreement, with $\kappa = 0.79$ with a 95% CI [0.77,0.82]), $\kappa = 0.77$ with a 95% CI [0.74,0.80]), and $\kappa = 0.77$ with a 95% CI [0.74,0.80]), respectively, whereas, pix2pix displayed a near-perfect agreement, with $\kappa = 0.85$ with a 95% CI [0.83,0.88]).

III. METHODS

Mouse Model: We used a standard streptozotocin (STZ) treated mouse model[11], as detailed in our earlier publication[12]. All animal studies were performed in accordance with protocols approved by the Institutional Animal Care and Use Committee at University at Buffalo. They were also consistent with federal guidelines and regulations, and followed the recommendations of the American Veterinary Medical Association guidelines on euthanasia. Renal tissue sections from 7 control and 7 STZ-treated mice were used (categorized as mild (200-400 mg/dL) or moderate DM (> 400 mg/dL)), which were formalin fixed and paraffin embedded (FFPE).

Tissue staining and imaging protocol: The FFPE sections were deparaffinized with an automated instrument, Discovery Ultra (Ventanta Medical Systems, Inc., Tucson, AZ). Subsequently, antigen retrieval was performed using an EDTA-based buffer. The tissue sections were spotted with DAPI mounting media (Vectashield Antifade Mounting Medium with DAPI, ex/em (nm): 358/461; Vector Laboratories, Inc., Burlingame, CA). The podocytes and PECs were labeled using WT1 (ab89901, Abcam, Cambridge, UK) as a primary antibody with Alexa Fluor 594 (ex/em (nm): 590/617) goat anti-rabbit IgG (1:1000, Life Technologies, Carlsbad, CA) as the secondary antibody. The slides were imaged for fluorescence at 40X magnification (0.13 µm/pixel) using an Aperio VERSA digital whole slide scanner (Leica Biosystems, Buffalo Grove, IL). Following fluorescence imaging, the slides were prepared for post-staining via PAS. Slides were soaked in xylene for about an hour, until the edge of the coverslip could gently be lifted with a knife. Once the coverslip was removed, the tissues were rehydrated. Rehydration consisted of 2x 10 min washes in xylene, followed by 2x 10 min washes in 100% ethanol, before stepping down with 2x 5 min washes in 70% ethanol, and then submerging the slides in ddH2O. A PAS Stain Kit (ab150680, Abcam, Cambridge, UK) was used to post stain the tissues. The slides were again imaged in brightfield mode at 40X magnification with the Aperio VERSA system.

Schematic overview: The PAS-stained WSI was fed to our H-AI-L pipeline[7] to extract the glomerulus locations (Figure 4a-b). Next, the PAS-stained WSI was aligned with the corresponding IF-stained WSI via image registration[6] (Figure 4c-d). Subsequently, 256 × 256 image patches containing glomeruli were extracted from the PAS and the corresponding IF WSI (Figure 4e-f) to train and test the pix2pix conditional GAN[5]. Once trained, extracted glomeruli image patches from the hold-out

Downloaded From: https://www.spiedigitallibrary.org/conference-proceedings-of-spie on 13 Dec 2022
Terms of Use: https://www.spiedigitallibrary.org/terms-of-use

mouse were fed to the network, which were then translated into *in silico* IF image patches (Figure 4g-j), which then underwent morphological processing[8] to extract WT1-positive cell boundaries, which were displayed along with input PAS WSIs (Figure 4k).

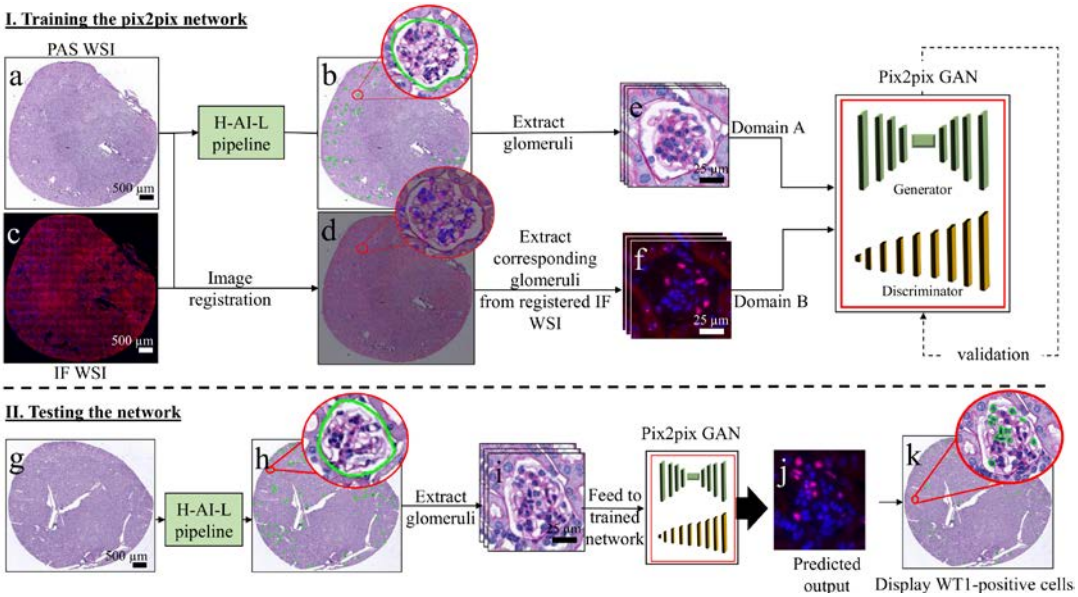

Figure 4. Schematic overview of the pipeline. a) Whole-slide image (WSI) of periodic acid-Schiff (PAS)- stained renal tissue section. b) Glomeruli detection by H-AI-L algorithm. c) WSI of the same section stained with IF markers. d) Result of image registration. e-f) Extraction of glomeruli image patches (from PAS and registered IF WSI), which were used to train the pix2pix network. g) Hold-out PAS WSI. h) Glomeruli detection by H-AI-L algorithm. i) Extraction of glomeruli patches, which were fed to the trained network for prediction. j) *In silico* IF image. k) WT1-positive cell boundaries displayed along Figure 4g.

Image registration and glomeruli detection: The four corners of the bounding box containing the tissues (PAS and IF), and their centroids, were used as landmark points for registration[6]. Manual offset values were added, if necessary, to obtain perfect registration.

To detect glomeruli in PAS-stained WSIs, all glomeruli were manually annotated in three randomly chosen PAS WSIs, and were used to train the H-AI-L algorithm[7], a convolutional neural network (CNN) trained to automatically segment glomeruli from brightfield WSIs of renal tissue sections.

Pix2pix GAN training and validation: The model was trained via leave-one-out validation, wherein all the glomerular image patches from one mouse were treated as hold-out cases and trained on the rest, with each of the 14 mice treated as a hold-out case in sequence. The training set for the pix2pix GAN architecture[5] consisted of ~1.4K paired image patches (PAS and IF), augmented into ~11K images by standard image augmentation techniques like flipping and rotation. Our model was trained for 20 epochs on an NVIDIA GeForce GTX GPU, based on the PyTorch implementation and hyperparameters specified by Isola et al[5].

WT1-positive cell segmentation and comparison with hand-segmented ground truth: In order to extract the WT1-positive cells from IF images, color deconvolution[13], morphological processing, and watershed algorithm[14] were used[8]. For image patches with staining artifacts, hand-segmented masks of WT1-positive cells were obtained.

Statistical analysis: To compare the performances of the pix2pix network and the expert annotators to the ground truth, linear-weighted Cohen's kappa[10] was calculated. Kappa < 0, 0-0.21, 0.21-0.4, 0.41-0.6, 0.61-0.8, and 0.81-1 indicated none, slight, fair, moderate, substantial, and near perfect

Downloaded From: https://www.spiedigitallibrary.org/conference-proceedings-of-spie on 13 Dec 2022
Terms of Use: https://www.spiedigitallibrary.org/terms-of-use

agreement, respectively. Additionally, Pearson's correlation coefficient was used to compute the association between the counts extracted from the *in silico* IF images (and the expert annotators) and the ground truth. To quantify the agreement between the ground truth and estimated WT1-positive cell counts, the Bland-Altman[9] plot was utilized.

IV. DISCUSSION

The automated detection of podocytes and PECs in brightfield images of renal tissue sections could enable not only rapid quantification of these cells, but also would aid in tracking disease progression. Our pipeline is a reproducible and accurate method for automated detection of WT1-positive cells in brightfield WSIs of renal tissue sections.

V. CONCLUSION AND FUTURE WORK

Our proposed framework based on careful generation of multi-modal microscopy image data and pix2pix conditional GAN, can be used as a generalized framework to detect important cellular compartments from digital histology images. This framework can be extended to other applications in digital pathology.

REFERENCES

1 Asanuma, K. & Mundel, P. The role of podocytes in glomerular pathobiology. *Journal of Clinical and Experimental Nephrology* **7**, 255-259 (2003).

2 Nagata, M. Podocyte injury and its consequences. *Kidney international* **89**, 1221-1230 (2016).

3 Lin, J. S. & Susztak, K. Podocytes: the weakest link in diabetic kidney disease? *Current diabetes reports* **16**, 45 (2016).

4 Appel, D. *et al.* Recruitment of podocytes from glomerular parietal epithelial cells. *Journal of the American Society of Nephrology* **20**, 333-343 (2009).

5 Isola, P., Zhu, J.-Y., Zhou, T. & Efros, A. A. in *Proceedings of the IEEE conference on computer vision and pattern recognition.* 1125-1134.

6 Modersitzki, J. *FAIR: flexible algorithms for image registration*. Vol. 6 (Siam, 2009).

7 Lutnick, B. *et al.* An integrated iterative annotation technique for easing neural network training in medical image analysis. *Nature machine intelligence* **1**, 112-119 (2019).

8 Gonzalez, R. C., Woods, R. E. & Masters, B. R. Digital image processing third edition. *Pearson International Edition* (2008).

9 Giavarina, D. Understanding bland altman analysis. *Biochemia medica: Biochemia medica* **25**, 141-151 (2015).

10 Cohen, J. Weighted kappa: nominal scale agreement provision for scaled disagreement or partial credit. *Psychological bulletin* **70**, 213 (1968).

Downloaded From: https://www.spiedigitallibrary.org/conference-proceedings-of-spie on 13 Dec 2022
Terms of Use: https://www.spiedigitallibrary.org/terms-of-use

11 Tesch, G. H. & Allen, T. J. Rodent models of streptozotocin-induced diabetic nephropathy (Methods in Renal Research). *Nephrology* **12**, 261-266 (2007).
12 Simon, O., Yacoub, R., Jain, S., Tomaszewski, J. E. & Sarder, P. Multi-radial LBP features as a tool for rapid glomerular detection and assessment in whole slide histopathology images. *Scientific reports* **8**, 1-11 (2018).
13 Ruifrok, A. C. & Johnston, D. A. Quantification of histochemical staining by color deconvolution. *Analytical and quantitative cytology and histology* **23**, 291-299 (2001).
14 Meyer, F. Topographic distance and watershed lines. *Signal processing* **38**, 113-125 (1994).

Downloaded From: https://www.spiedigitallibrary.org/conference-proceedings-of-spie on 13 Dec 2022
Terms of Use: https://www.spiedigitallibrary.org/terms-of-use